Molecular Biology of the Cell
Vol. 15, 4310–4320, September 2004

Myofibroblast Development Is Characterized by Specific Cell-Cell Adherens Junctions[V]

B. Hinz,*† P. Pittet,* J. Smith-Clerc,* C. Chaponnier,‡ and J.-J. Meister*

*Laboratory of Cell Biophysics, Swiss Federal Institute of Technology, 1015 Lausanne, Switzerland; and ‡Department of Pathology and Immunology, Centre Medical Universitaire, University of Geneva, 1211 Geneva 4, Switzerland

Submitted May 11, 2004; Revised June 25, 2004; Accepted June 29, 2004
Monitoring Editor: Paul Matsudaira

Myofibroblasts of wound granulation tissue, in contrast to dermal fibroblasts, join stress fibers at sites of cadherin-type intercellular adherens junctions (AJs). However, the function of myofibroblast AJs, their molecular composition, and the mechanisms of their formation are largely unknown. We demonstrate that fibroblasts change cadherin expression from N-cadherin in early wounds to OB-cadherin in contractile wounds, populated with α-smooth muscle actin (α-SMA)-positive myofibroblasts. A similar shift occurs during myofibroblast differentiation in culture and seems to be responsible for the homotypic segregation of α-SMA-positive and -negative fibroblasts in suspension. AJs of plated myofibroblasts are reinforced by α-SMA–mediated contractile activity, resulting in high mechanical resistance as demonstrated by subjecting cell pairs to hydrodynamic forces in a flow chamber. A peptide that inhibits α-SMA–mediated contractile force causes the reorganization of large stripe-like AJs to belt-like contacts as shown for enhanced green fluorescent protein-α–catenin-transfected cells and is associated with a reduced mechanical resistance. Anti-OB-cadherin but not anti-N-cadherin peptides reduce the contraction of myofibroblast-populated collagen gels, suggesting that AJs are instrumental for myofibroblast contractile activity.

INTRODUCTION

Fibroblast-to-myofibroblast modulation represents a crucial step in wound granulation tissue contraction and in the production of the connective tissue deformations typical of fibrocontractive diseases (Serini and Gabbiani, 1999; Tomasek *et al*., 2002). Hallmarks of myofibroblast differentiation are the development of stress fibers (Gabbiani *et al*., 1971) and the de novo expression of α-smooth muscle actin (α-SMA) (Skalli *et al*., 1986; Darby *et al*., 1990). Incorporation of α-SMA into stress fibers confers to myofibroblasts a high contractile activity (Hinz *et al*., 2001a), leading to the formation of specialized contacts with the extracellular matrix (ECM) (Hinz *et al*., 2003) that are called supermature focal adhesions (FAs) in vitro (Dugina *et al*., 2001) and fibronexus in vivo (Singer *et al*., 1984). The high contractile activity of α-SMA is inhibited by cytoplasmic delivery of the α-SMA-specific N-terminal sequence AcEEED (Chaponnier *et al*., 1995) as a membrane-penetrating fusion peptide (SMA-FP) (Hinz *et al*., 2002) that also blocks the formation of supermature FAs (Hinz *et al*., 2003). At the interface between proteins of the ECM and intracellular stress fibers, supermature FAs contribute to the transmission of force and to the sensing of local tension, thus providing indirect cell–cell communication through fields of stress in the surrounding matrix (for review, see Hinz and Gabbiani, 2003b).

Stress fibers of contacting myofibroblasts also are directly connected at sites of cadherin-type cell-cell adherens junctions (AJs) that have been described ultrastructurally as dense plaques underlying the plasma membrane of fibroblasts in wound granulation and in fibrotic tissue; AJs are absent in normal tissue fibroblasts that do not develop stress fibers (Gabbiani and Rungger-Brandle, 1981; Welch *et al*., 1990). On the cytoplasmic side of AJs, actin filaments bind directly to α-catenin as part of a complex consisting the cytosolic proteins β-catenin, γ-catenin (plakoglobin), p120CTN, and the cytoplasmic domain of transmembrane cadherins (for reviews, see Nagafuchi, 2001; Wheelock and Johnson, 2003). The extracellular domains of two cadherins trans-interact with each other in a Ca^{2+}-dependent and generally homophilic manner (for reviews, see Gumbiner, 2000; Angst *et al*., 2001), although heterophilic interactions seem to occur frequently (Shimoyama *et al*., 2000) and have been described, for example, between cultured fibroblasts and epithelial cells (Volk *et al*., 1987; Omelchenko *et al*., 2001).

Like myofibroblasts in vivo, fibroblasts cultured on rigid planar substrates form stress fibers and develop AJs, which are generally thought to be transient and to mediate contact inhibition of movement and of cell division. N-cadherin (cad-2) seems to be the most commonly expressed cadherin in fibroblasts (Hatta and Takeichi, 1986; Geiger *et al*., 1990), which, however, were shown to express a variety of cadherins, including OB- (cad-11) (Hoffmann and Balling, 1995; Orlandini and Oliviero, 2001), R- (cad-4) (Shin *et al*., 2000),

Article published online ahead of print. Mol. Biol. Cell 10.1091/mbc.E04–05–0386. Article and publication date are available at www.molbiolcell.org/cgi/doi/10.1091/mbc.E04–05–0386.

[V] Online version of this article contains supporting material. Online version is available at www.molbiolcell.org.

† Corresponding author. E-mail address: boris.hinz@epfl.ch.

Abbreviations used: AJ, adherens junction; α-SMA, α-smooth muscle actin; EMT, epithelial-to-mesenchymal transition; FA, focal adhesion; FP, fusion peptide; LF, lung fibroblast; LPA, lysophosphatic acid; PFA, paraformaldehyde; SCF, subcutaneous fibroblast; SKA, skeletal actin; SMC, smooth muscle cell; TGFβ, transforming growth factor-β; TGFβ-sRII, recombinant soluble TGFβ receptor type II; TX-100, Triton X-100.

P-cadherin (cad-3) (Yonemura *et al*., 1995), and Fat (Matsuyoshi and Imamura, 1997) (for review, see Hinz and Gabbiani, 2003a). So far, no studies have been performed to systematically correlate the pattern of cadherin expression with specific fibroblast functions; in particular little is known about the molecular nature, the mechanisms of formation and the function of myofibroblast AJs in vivo and in vitro. Differentiated myofibroblasts share a number of similarities with smooth muscle cells (SMCs) (Tomasek *et al*., 2002), potentially including the expression of SMC-characteristic cadherins, such as R- (Rosenberg *et al*., 1997), T-cadherin (cad-13) (Ivanov *et al*., 2001), and cadherin 6B (Chimori *et al*., 2000) (for review, see Moiseeva, 2001). Acquisition of a specific cadherin pattern in myofibroblasts may be induced by transforming growth factor-β (TGFβ), the major promoter of myofibroblast differentiation (Desmouliere *et al*., 1993; Ronnov-Jessen and Petersen, 1993), which induces the expression of a variety of proteins during fibroblast–myofibroblast transition (Malmstrom *et al*., 2004). A similar TGFβ-induced switch occurs during epithelial-to-mesenchymal transition (EMT) from E-cadherin–expressing epithelial cells to N-cadherin–expressing fibroblastic cells (Miettinen *et al*., 1994; Bhowmick *et al*., 2001).

Here, we have shown that during wound healing in vivo and after TGFβ induction in vitro, myofibroblast differentiation is accompanied by an increase of OB-cadherin expression and a decrease of N-cadherin expression. Myofibroblast AJs are reinforced by the high contractile activity mediated by incorporation of α-SMA into stress fibers and, in turn, provide high mechanical resistance to extracellularly applied forces. Such stabilized contacts seem to improve force development of myofibroblast populations in three-dimensional collagen gels. It is conceivable that AJs couple the stress fibers of adjacent myofibroblasts to coordinate their contractile activity during connective tissue remodeling. In addition, a specific cadherin expression pattern may serve as a marker and/or modulator of the differentiation state of fibroblasts and AJs represent a potential therapeutic target for the treatment of fibrocontractive diseases.

MATERIALS AND METHODS

Cell Culture and Drugs

Primary fibroblasts explanted from rat lung (LF) and subcutaneous tissue (SCF), lineage rat embryonic fibroblasts (REF-52) and primary rat vascular SMCs (Bochaton-Piallat *et al*., 1996) were obtained and cultured as described previously (Hinz *et al*., 2003). Fibroblasts were generally grown for 5 d in control conditions, in the presence of TGFβ1 (5 ng/ml; R&D Systems, Minneapolis, MN) to induce myofibroblast differentiation or of the TGFβ-antagonizing recombinant soluble Fc:TGFβ receptor type II (TGFβ-sRII, 1 μg/ml; gift of Biogen, Cambridge, MA). Fusion peptides (FPs), consisting of a cell-penetrating vector (Derossi *et al*., 1994) and the α-SMA N-terminal sequence AcEEED (SMA-FP) (Chaponnier *et al*., 1995) or the α-skeletal actin N-terminal AcDEDE (SKA-FP), respectively, were produced as described previously (Hinz *et al*., 2002) and used at 5 μg/ml. Cell contraction was modulated by Y27632 (10 μM; Yoshitomi Pharmaceutical Industries, Osaka, Japan), fasudil (10 μM, HA1077; Calbiochem, San Diego, CA), 2,3-butanedione monoxime (BDM, 10 μM), ML-7 (30 μM), lysophosphatic acid (LPA, 10 μM), and staurosporin (50 nM) (all Sigma Chemical, Buchs, Switzerland); cytochalasin D (Sigma Chemical) was used at 1 μM. Cadherin binding was inhibited generally by chelating Ca^{2+} with 2 mM EGTA and specifically with function-blocking peptides anti-N-cadherin (ADH126), anti-OB-cadherin (ADH113), and compared with respective control peptides (ADH135 and ADH114) (Cadherin Biomedical, Ottawa, Ontario, Canada) at 1 mg/ml.

Animal Experiments

A total of 15 female Wistar rats (200–220 g) was used; after shaving the skin, full thickness 25 × 25-mm wounds, including the cutaneous muscle, were made using surgical scissors in the middle of the dorsum on the first day of the experiments and were allowed to heal spontaneously. Rats were sacrificed by CO_2 anesthesia, and granulation tissue was harvested every third day 3–12 d postwounding as described previously (Hinz *et al*., 2001b).

Enhanced Green Fluorescent Protein (EGFP) Constructs and Time-Lapse Videomicroscopy

SCFs and REF-52 were transfected with EGFP-α-catenin (a kind gift of Dr. Kaibuchi, Nagoya University, Aichi, Japan) (Fukata *et al*., 2001) and N-cadherin-EGFP (a kind gift of Dr. Gauthier-Rouviere (Centre National de la Recherche Scientifique, Montpellier, France) (Mary *et al*., 2002), by using FuGENE 6 (Roche Diagnostics, Reinach, Switzerland) according to the manufacturer's protocol. Cells were cultured for minimum 4 d in medium/10% fetal calf serum (FCS) ($\pm$TGFβ) on glass observation chambers (Hinz *et al*., 2003) and were recorded live in serum-free F-12 medium; serum depletion showed no effect on AJ dynamics during 5 h of recording. Cells were observed with an inverted microscope (Axiovert 135; Carl Zeiss, Feldbach, Switzerland), equipped with a heating stage and CO_2 incubation chamber (Carl Zeiss), EGFP- and neutral density filter set (Omega Optical, Brattleboro, VT) and a digital charge-coupled device camera (Hamamatsu C4742-95–12ERG; Bucher Biotech, Basel, Switzerland). Movies were acquired with Openlab 3.1.2 software (Improvision, Basel, Switzerland) in intervals of 1 frame/min.

Fibroblast Aggregation

To assess cadherin-mediated binding affinities, fibroblasts were washed with Hank's balanced salt solution (HBSS), containing 2 mM $CaCl_2$ (HBSS/Ca^{2+}), detached with 0.25% trypsin solution plus 2 mM Ca^{2+} (trypsin/Ca^{2+}) for 30 min and resuspended at 50,000 cells/ml in a 1:1 mixture of HBSS/$Ca^{2+}$and minimal essential medium/5%FCS/Ca^{2+}. Aggregated cells were thoroughly dispersed by repeated pipetting; α-SMA–positive and –negative fibroblasts were then mixed 1:1 and were either seeded immediately to test initial cell dispersion or after rotating the suspension in tubes at 70 rpm at 37°C for 60 min in the presence of 2 mM Ca^{2+} to assess formation of aggregates. After 2-h plating, cells were immunostained for β-catenin, α-SMA, and DNA (see below) and documented with a 10× objective (Fluar, numerical aperture [NA] 0.5; Carl Zeiss). Composition and size of formed aggregates was automatically quantified using a self-developed journal in MetaMorph image analysis software (Universal Imaging, Downingtown, PA). Briefly, the boundaries of individual aggregates were transformed into regions of interest by thresholding for β-catenin membrane fluorescence, and the number of cells within each identified aggregate was determined by counting the number of 4,6-diamidino-2-phenylindole (DAPI)-stained nuclei. The binary image of α-SMA fluorescence was then subtracted from the binary DAPI image, leaving only nuclei of α-SMA-positive cells, which were counted and divided by the total number of cells (=percentage of myofibroblasts per aggregate).

Flow Chamber Experiments

To test binding strength between suspended and plated cells, SCF ($\pm$TGFβ) was detached with trypsin/Ca^{2+} for 30 min, thoroughly resuspended at 200,000 cells/ml in HBSS/Ca^{2+}, and seeded on top of a confluent SCF monolayer, grown on a glass coverslip ($\pm$TGFβ) at the bottom of a parallel-plate perfusion chamber. Cells adhered 30 min at 37°C before the flow chamber was mounted on a microscope stage (Axiovert 135; Carl Zeiss) and attached to peristaltic pump; a Windkessel chamber (Verrerie Carouge, Geneva, Switzerland) was used to produce a constant flow of HBSS/Ca^{2+} (37°C). After gently removing nonattached cells, the flow rate was increased every minute in steps of 1 to 5 ml s^{-1}, corresponding to wall shear forces of up to 4 Nm^{-2}; digital movies were recorded at 1 frame/5 s with Openlab sofware (Improvision) by using a 10× Objective (Apochromat Ph1, NA 0.25; Carl Zeiss). The number of adhering cells at the end of each flow rate step was automatically determined with a threshold routine implemented in Scion Image (Scion, Frederick, MD), identifying round suspended cells by their strong halo in phase contrast and their characteristic size.

Antibodies, Immunofluorescence, and Confocal Microscopy

Cryostat sections of 3-μm-thickness were produced from frozen tissue (Hinz *et al*., 2001b). Cells were permeabilized for 5 min with 0.2% Triton X-100 (TX-100) in 3% paraformaldehyde (PFA) and fixed with 3% PFA/phosphate-buffered saline for 10 min. We used primary antibodies according to Table 1 and as secondary antibodies tetramethylrhodamine B isothiocyanate- and fluorescein isothiocyanate-conjugated goat anti-mouse IgG1 and IgG2a (Southern Biotechnology Associates, Birmingham, AL) and Alexa 488-, Alexa 568-, and Cy5-conjugated goat anti-mouse, goat anti-rabbit, and chicken anti-goat antibodies (Molecular Probes, Eugene, OR); F-actin was probed with phalloidin-Alexa 488 (Molecular Probes) and DNA with DAPI (Fluka, Buchs, Switzerland). Images were acquired as described for live imaging or with a confocal microscope (DM RXA2 with a laser scanning confocal head TCS SP2 AOBS; Leica, Glattbrugg, Switzerland), equipped with objective 40×/1.25 and 60×/1.4 (Leica). Figures were assembled with the use of Adobe Photoshop.

Cell Fractionation and Western Blot Analysis

Dissected tissues were snap-frozen in liquid nitrogen, crushed, and dissolved in sample buffer, sonicated, boiled for 3 min, and protein concentration was determined according to Bradford as described previously (Hinz *et al*., 2001b).

Table 1. Primary antibodies

No.	Protein	Host	MW	Provided by
(1)	α-catenin	rb IgG	102	ZY
(2)	α-SMA (αSM-1)	m IgG2a	42	Gabbiani (Skalli *et al.*, 1986)
(3)	β-catenin (CAT-15)	rb IgG	92	ZY
(4)	E-cadherin	m IgG2b	120	TL
(5)	K-cadherin (2B6)	m IgG	130	Schalken (Tomita *et al.*, 2000)
(6)	K-cadherin (cad-6)	rb IgG	130	Mège (Marthiens *et al.*, 2002)
(7)	M-cadherin	m IgG2a	130	TL
(8)	N-cadherin	m IgG1	130	TL
(9)	N-cadherin (H-63)	rb IgG	130	SC
(10)	OB-cadherin	rb IgG	110	Mège (Marthiens *et al.*, 2002)
(11)	OB-cadherin (C16)	g IgG	110	SC
(12)	OB-cadherin (cad-11)	m IgG1	110	Schalken (Tomita *et al.*, 2000)
(13)	p120CTN	m IgG1	120	TL
(14)	pan-cadherin	rb IgG	130, 120	ZY
(15)	pan-cadherin (C19)	g IgG	130, 120	SC
(16)	P-cadherin (H105)	rb IgG	120	SC
(17)	R-cadherin (H66)	rb IgG	120	SC
(18)	T-cadherin	rb IgG	105, 130	Resink (Niermann *et al.*, 2003)
(19)	T-cadherin (H126)	rb IgG	105, 130	SC
(20)	VE-cadherin (C-19)	g IgG	130	SC
(21)	Vimentin (V-9)	m IgG1	57	Dako Cytomation, Denmark NS

ZY, Zymed Laboratories (Stehelin & Cie AG, Basel, Switzerland); SC, Santa Cruz (Heidelberg, Germany); TL, BD Transduction Laboratories (Lexington, KY). Other antibodies are kind gifts from Drs. T. Resink (University Hospital, Basel, Switzerland), J.A. Schalken (University Hospital Nijmegen, The Netherlands), and R.M. Mège (Institut National de la Santé et de la Recherche Médical, Paris, France). MW, apparent molecular weight in Western blots; g, goat; rb, rabbit; m, mouse.

To assess association of proteins with the TX-100–insoluble cytoskeleton of cultured cells, cytosolic proteins were extracted for 2 × 5 min with ice-cold extraction buffer (0.5% TX-100, 60 mM PIPES, 25 mM HEPES, 10 mM EGTA, 2 mM $MgCl_2$, 1 mM Na-orthovanadate, pH 6.9), supplemented with protease inhibitors (Complete-EDTA, Roche Diagnostics, Mannheim, Germany) as described previously (Hinz *et al.*, 2003). Remaining TX-100–insoluble cytoskeletal proteins were scraped from the culture dish and suspended in the same volume of extraction buffer. Fractions and total cell lysates were run on 10% SDS-minigels (Bio-Rad, Glattbrugg, Switzerland), blotted, and proteins were probed with the same primary antibodies as used in immunofluorescence. Horseradish peroxidase-conjugated secondary antibodies goat anti-mouse IgG and goat anti-rabbit IgG (Jackson ImmunoResearch Laboratories, West Grove, PA) were detected by enhanced chemiluminescence (Amersham, Rahn AG, Zürich, Switzerland). For quantification of blots, bands were digitized with a scanner (Epson 2450 Photo, Dietlikon, Switzerland), and the ratio between all band densities of one blot was calculated by computer software (ImageQuant version 3.3; Amersham Biosciences, Piscataway, NJ); equal loading was tested by probing vimentin expression (clone V9; DakoCytomation Denmark A/S, Glostrup, Denmark), which serves as a fibroblast housekeeping protein. The quantified vimentin signal was generally used to normalize signals from other proteins, as described previously (Hinz *et al.*, 2001b).

Stressed Collagen Lattice Contraction

SCFs were grown at 1.75×10^5 cells/ml in attached collagen lattices (0.75 mg/ml rat tail collagen I; First Link, Birmingham, United Kingdom) for 5d (±TGFβ); gels were then released and diameter reduction after 30 min was expressed as percentage of contraction as described previously (Hinz *et al.*, 2001a). Anti-cadherin peptides were added 3 h before gel release.

Statistical Analysis

Mean values are presented ± SD and tested by a two-tailed heteroscedastic Student's *t* test. Differences were considered to be statistically significant at $p \leq 0.05$, indicated by an asterisk (*) and marked with a double asterisk (**) for $p \leq 0.001$.

RESULTS

Expression of AJ Proteins Is Up-Regulated in Fibroblasts during Dermal Wound Healing

To evaluate the time course of AJ formation in fibroblasts and to characterize their molecular composition during the course of wound healing, we have analyzed AJ protein expression in 3- to 12-d-old granulation tissue of spontaneously healing full thickness rat wounds. Fibroblasts in normal dermis exhibited no detectable levels of AJ proteins (unpublished data). Correlating with the formation of microfilament bundles ~6 d after wounding (Hinz *et al.*, 2001b), we observed de novo expression of AJ markers β- and α-catenin in granulation tissue fibroblasts (Figure 1, A and F) in conjunction with a significant increase in cadherin expression, as assessed using pan-cadherin antibodies (Figure 1F). AJ formation clearly preceded myofibroblast differentiation and α-SMA expression that exhibited a peak ~9 d postwounding (Figure 1, B and F); at this stage, the levels of α- and β-catenin were highest (Figure 1F). AJ proteins showed as punctuate staining in immunofluorescence and were associated with actin filament bundles (Figure 1B, inset); AJ protein expression decreased at wound closure with decreasing α-SMA expression 12 d postwounding; Figure 1C). The only cadherins that were considerably up-regulated in granulation tissue fibroblasts during wound healing seemed to be N- and OB-cadherin; moreover, we detected high levels of T-cadherin (Figure 1F). K- (Table 1, 5), R- (Table 1, 17), and M-cadherin (Table 1, 7) (unpublished data) were expressed at detection level and were attributed to fibroblasts by coimmunostaining for vimentin; they did not change significantly during wound healing. VE- or E-cadherin were not expressed in fibroblasts but were expressed in endothelial and epidermal cells, respectively (unpublished data). Interestingly, the cadherin pattern changed with myofibroblast differentiation; in particular, N-cadherin reached an expression peak after 6 d (Figure 1, D and F), whereas OB-cadherin was up-regulated only later ~9 d postwounding (Figure 1, E and F), resulting in a threefold increase of the OB-/N-cadherin ratio from

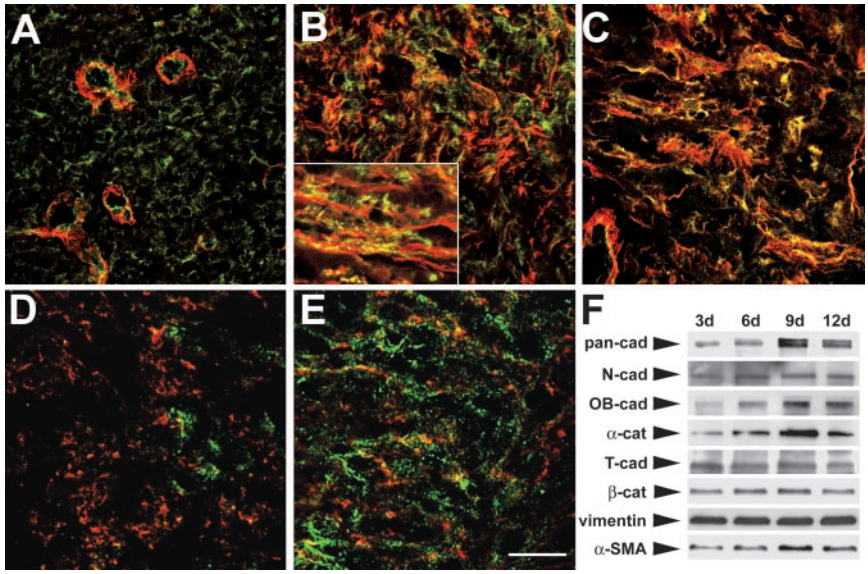

Figure 1. AJ development during myofibroblast differentiation in wound granulation tissue. (A–F) Sections of 6-d- (A and D), 9-d- (B and E), and 12-d-old (C) granulation tissue from full thickness rat wounds were costained for α-SMA (red) and β-catenin (green) (A–C) or N- (red) and OB-cadherin (green) (D and E); images were reconstructed from three laser scanning optical sections of 0.2 μm. Bar, 10 μm (A–E), 20 μm (inset, B). (G) Equal protein amounts from extracts from 3-to 12-d-old granulation tissue were blotted, and vimentin expression was quantified by densitometric analysis and used to equilibrate protein levels accordingly, followed by blotting again for cytoskeletal and AJ proteins. Protein loads and cadherin antibodies according to Table 1: 30 μg (1, 8, 12, 14, and 18), and 15 μg (all others). Presented blots are generated from one series of wound samples (3–12 d) and are representative for three independently collected series.

~0.6 after 6 d to ~1.9 after 12 d as quantified by densitometric analysis.

AJ Characteristics Change during Fibroblast to Myofibroblast Transition in Culture

Using cultured primary LFs and SCFs and lineage REF-52 cells, we have first characterized the change in AJ morphology and molecular composition upon modulation of myofibroblast differentiation. Control SCF (~15% α-SMA positive) formed small and stripe-like AJs of 2–5 μm in length at the junction of α-SMA-negative stress fibers (Figure 2A). TGFβ induced myofibroblast differentiation (~85% α-SMA-positive) and caused elongation of AJs to 20–30 μm at the terminal portion of α-SMA–positive stress fibers (Figure 2B). A similar AJ morphology was observed in LF and REF-52, both containing constitutively high proportions of α-SMA–positive cells (~85%; unpublished data); TGFβ-sRII reduced α-SMA expression in these cells to ~10% and AJ size to the level of control SCFs (Figure 2A).

In contrast to what was observed during granulation tissue development, the expression levels of α- and β-catenin were down-regulated during fibroblast–myofibroblast transition. Systematic evaluation by Western blotting revealed the expression of a variety of cadherins in fibroblasts, of which OB-, T- (Figure 2F), K-, P-, and R-cadherin (unpublished data) were up-regulated by TGFβ and were expressed in vascular SMCs, whereas N-cadherin was down-regulated and absent from SMCs (Figure 2F). AJs between α-SMA–negative primary fibroblasts exhibited predominant expression of N-cadherin (Figure 2C), whereas AJs of α-SMA–positive myofibroblasts contained high levels of OB-cadherin either exclusively (Figure 2, C and D) or in colocalization with N-cadherin (Figure 2, C and D, arrowheads). K-, P-, and R-cadherin occurred in low levels in AJs and were not differently distributed before and after TGFβ treatment; T-cadherin homogeneously localized to the cell membrane and never to AJs (unpublished data).

To evaluate the function of different cadherin expression patterns in fibroblast and myofibroblast cell–cell recognition, we mixed suspensions of α-SMA–positive (+TGFβ) and –negative (+TGFβ-sRII) SCFs and evaluated the percentage of α-SMA–expressing cells in the aggregates by immunostaining. Plating fibroblasts immediately after mixing demonstrated a good initial cell separation and equal numbers of α-SMA–positive and –negative cells (Figure 3A). After incubation in rotating tubes, aggregates were formed in Ca^{2+}-containing medium (Figure 3B) but not in the presence of 2 mM EGTA (unpublished data), indicating formation of Ca^{2+}-dependent cadherin-type AJs. Most aggregates were predominantly composed of either α-SMA-positive or -negative fibroblasts (Figure 3E), demonstrating homotypic segregation of both cell types. Aggregates containing $\leq$30% α-SMA–negative cells (Figure 3E, green) were significantly larger (16.3 $\pm$ 7.2 cells; Figure 3, C and F) compared with those containing $\leq$30% α-SMA–positive cells (7.4 $\pm$ 3.1 cells; Figure 3, F and E, green). Similar results were obtained using LFs. After 2 h of plating, myofibroblasts exhibited few α-SMA filament bundles (Figure 3D), and AJs were morphologically indistinguishable from that of fibroblasts (Figure 3C). Segregation of suspended fibroblasts relied solely on their surface properties, because aggregate formation was not affected by depolymerizing F-actin with cytochalasin D, by inhibiting cell contraction with ROCK inhibitor Y27632 or by inhibiting α-SMA–mediated contractile activity by using the SMA-FP (unpublished data).

Myofibroblast Differentiation Coincides with AJ Stabilization and Increased Mechanical Resistance

One possible function for myofibroblast AJs is the intercellular transmission of α-SMA–mediated contractile force, which requires mechanically resistant contacts. Thus, we tested the stabilization of AJ proteins with stress fibers by blotting TX-100–insoluble cytoskeletal fractions (Figure 4A). In all cell types tested, the fraction of TX-100–insoluble AJ proteins moderately (β-catenin and N-cadherin) or strongly (OB-cadherin) increased during fibroblast to myofibroblast transition. By normalizing to the decreasing total protein levels of β-catenin and N-cadherin (Figure 2E) upon myofibroblast differentiation, a clear redistribution of AJ proteins to the cytoskeletal fraction was demonstrated (Figure 4B), indicating a recruitment into F-actin–associated AJs.

We further evaluated the mechanical resistance of contacts formed between suspended and plated fibroblasts (F) and myofibroblasts (M) in a parallel-plate flow chamber. Within 10 min, suspended cells formed AJs with the dorsal membrane of spread cells (unpublished data) and started to

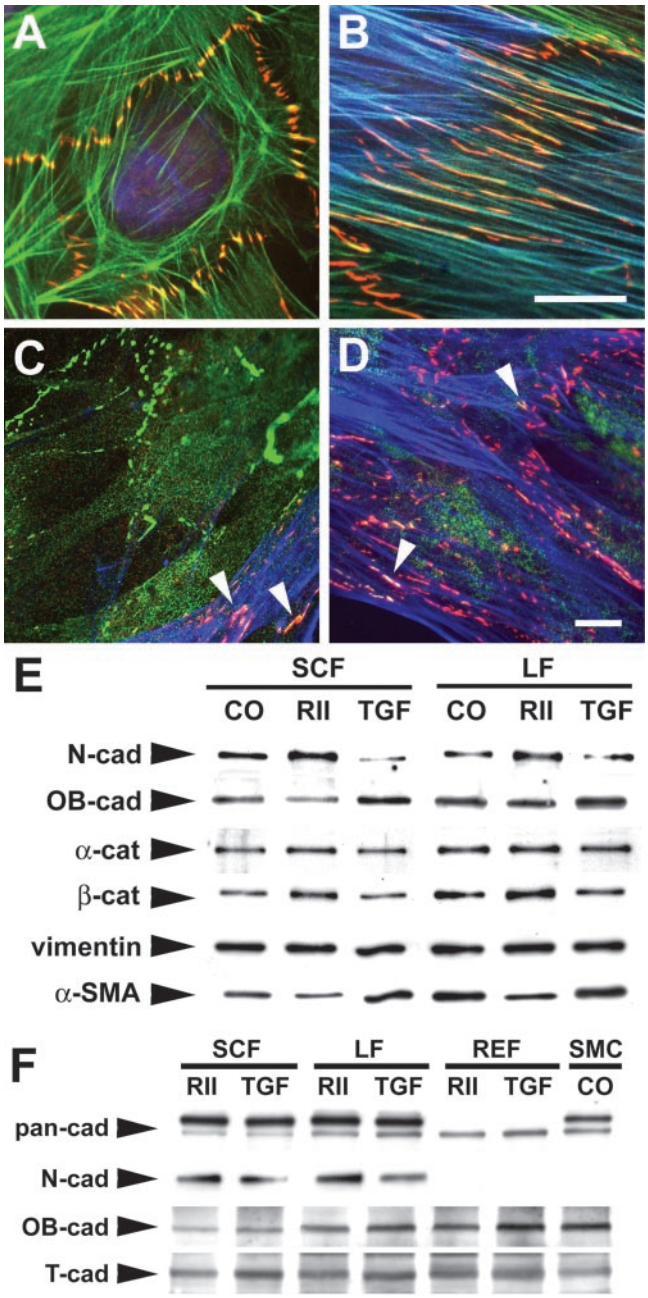

Figure 2. AJs are modified during myofibroblast differentiation in culture. (A–D) SCFs were grown for 5 d without (A and C) and with TGFβ (B and D) and costained for β-catenin (red) and F-actin (phalloidin, green) (A and B) or N- (green) and OB-cadherin (red) (C and D). Differentiated myofibroblasts were identified by expression of α-SMA (blue); arrowheads indicate colocalization of N- and OB-cadherin. Bars, 25 μm. (E and F) Total lysates of SCFs, LFs, and REF-52, grown for 5 d in control medium (CO), in the presence of TGFβ (TGF) or of TGFβ-sRII (RII) and vascular SMCs were blotted for cytoskeletal and AJ proteins. Anti-cadherin antibodies used in E: 9 and 11; in F, similar to Figure 1; protein loads: 5 μg (1, 8, 9, 11, 12, and 14), and 2.5 μg (all others).

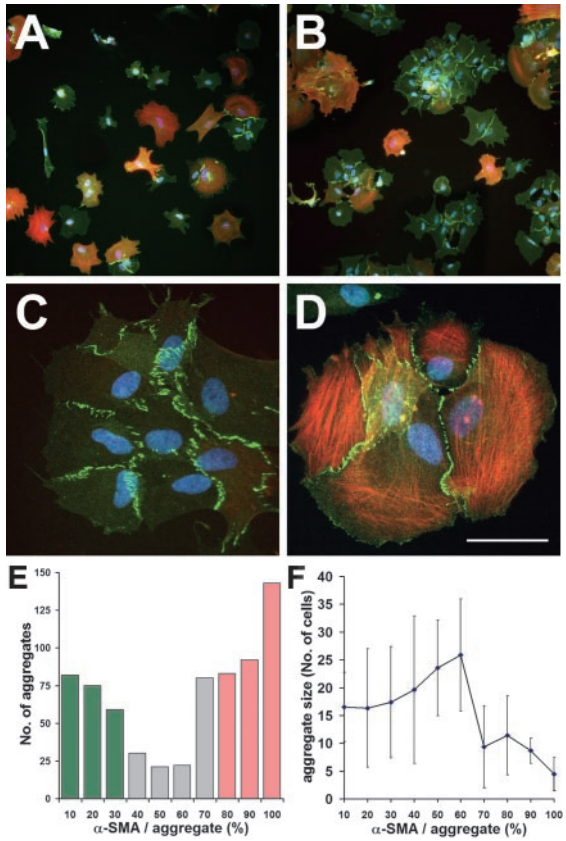

Figure 3. α-SMA–positive and –negative fibroblasts segregate in suspension. TGFβ-treated and control SCFs were suspended, mixed, and plated for 2 h either immediately (A) or after 60-min rotated incubation (B–D) and stained for α-SMA (red), β-catenin (green), and nuclei (DAPI, blue). Bar, 50 μm (C and D), 150 μm (A and B). Stained samples were used to calculate the number (E) and mean size (F) of aggregates, classified by the percentage of α-SMA–positive cells per aggregate. Data are presented from three independent pooled experiments; error bars indicate SD of mean. Green bars indicate that maximum 30% of cells per aggregate are α-SMA–negative (green), red bars signify maximum 30% of α-SMA–positive cells per aggregate and gray bars indicate "mixed" aggregates, where 31–70% of the cells per aggregate are α-SMA positive.

organize these contacts within 30 min (Figure 5A) as schematized in Figure 5B. In homo-cellular pair combinations, increasing the shear force to 2.9 Nm^{-2} reduced the percentage of adherent fibroblasts to 51 $\pm$ 6% (Figure 5C, F on F, $\diamond$), compared with 74 $\pm$ 3% of adherent myofibroblasts (Figure 5C, M on M, $\square$). Myofibroblast AJs resisted even higher forces of 3.9 Nm^{-2} and cells ripped off at the plasma membrane in contrast to a separation at the cell-cell contact area as observed for fibroblasts (unpublished data). Interestingly, in hetero-cellular combinations at medium shear force (1.9 Nm^{-2}), suspended fibroblasts showed stronger adhesion to spread myofibroblasts (Figure 5D, F on M, $\bigcirc$) compared with the inverse situation (Figure 5D, M on F, $\triangle$). Inhibition of α-SMA contractile activity by adding SMA-FP reduced fibroblast adhesion to spread myofibroblasts (F on M, Figure 5D, $\bullet$) and of homo-cellular myofibroblast pairs (M on M; unpublished data) to the level of fibroblast-to-fibroblast adhesion; however, SMA-FP was without effect on myofibroblast attachment to spread fibroblasts (Figure 5D, M on F, $\blacktriangle$) and on homo-cellular fibroblast pairs (F on F; unpublished data). These results indicate that organization of α-SMA into contractile bundles, which occurs in spread but not in suspended cells (Figure 5B), plays an important role in reinforcing AJs.

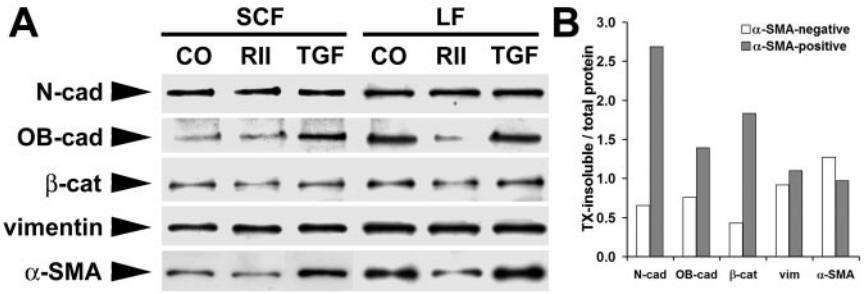

Figure 4. Stabilization of AJ proteins with the cytoskeleton increases with myofibroblast differentiation. (A) SCFs and LFs were grown for 5 d in control medium (CO), in the presence of TGFβ (TGF) and TGFβ-sRII (RII). TX-100–insoluble fractions were prepared and blotted for AJ proteins and α-SMA; vimentin was used as loading control. (B) TX-100–insoluble protein was quantified by densitometry and normalized to the pooled TX-100–insoluble and –soluble fractions (=total protein) of TGFβ- (α-SMA–positive) and TGFβ-sRII treated (α-SMA–negative) SCFs.

To further investigate the role of α-SMA in AJ formation and reinforcement, we have transfected SCF and REF-52 with EGFP-tagged N-cadherin (Mary *et al*., 2002) and α-catenin (Fukata *et al*., 2001) and observed AJ dynamics by live videomicroscopy. Both EGFP-tagged proteins localized to AJs that were large, stripe-like, and persisted over several hours in TGFβ-induced myofibroblasts (Figure 6A, x-50′-0′, Fig 6video1.mov). Treatment with SMA-FP visibly relaxed cells after ~15 min, and AJs were reorganized within 30 min to a continuous line at the cell-cell junction (Figure 6A, 30′) that gradually lost EGFP fluorescence intensity (Figure 6A, 50′); the control SKA-FP was always without effect (Figure 6B). After 2-h SMA-FP treatment, AJs were reduced to small point-like structures that lined up at the junctions of virtually all cells in the treated population (Figure 6C); this reduction in AJ size correlated with a decrease of AJ proteins in the TX-100–insoluble cytoskeletal fraction (Figure 6F). The effect of SMA-FP on AJs was comparable with a general inhibition of cell contraction by using Y27632 (Figure 6Dl; Fig 6video2.mov), BDM, ML-7, and HA1077 (unpublished data); inducing contraction and stress fiber formation with LPA (Figure 6E; Fig 6video3.mov) and staurosporin (unpublished data) reinforced AJ compared with control (Figure 6B). Hence, α-SMA seems to play an important role in stabilizing myofibroblast AJs by mechanically reinforcing cell–cell contacts.

OB-Cadherin Incorporation in AJs Improves Myofibroblast Contractile Activity

By connecting stress fibers intercellularly, AJs may improve the contractile activity of myofibroblasts in tissue. The classical way to inhibit AJ formation with EDTA was inappropriate to test the effect of AJs on cell contraction because Ca^{2+} removal increased contraction of fibroblast-populated collagen gels and of individual cells (unpublished data), presumably by interfering with signaling. Thus, we examined the effect of specific inhibitors of the most abundant myo/fibroblast cadherins, OB- and N-cadherin, on the contractile activity of control and TGFβ-treated SCF. Within 2 h, anti-N- and anti-OB-cadherin caused the complete and spe-

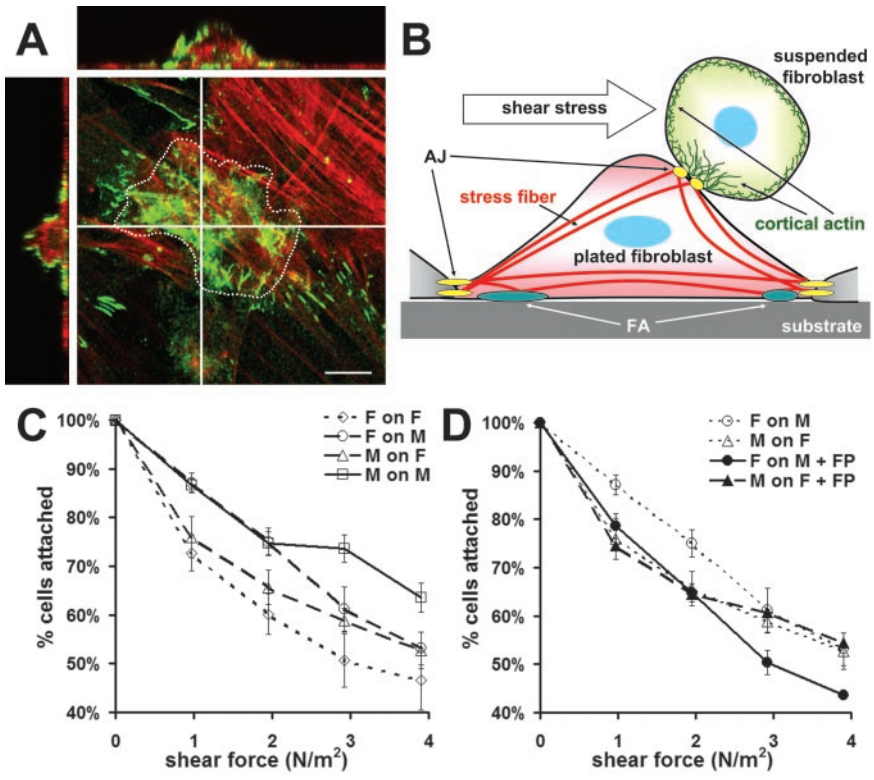

Figure 5. Myofibroblast AJs provide mechanical resistance. SCFs were grown for 5 d with TGFβ (M) and without (F) on the bottom of a parallel-plate flow chamber; similarly treated SCFs were seeded onto this cell monolayer and adhered for 30 min. (A) Cells were stained for α-SMA (red) and β-catenin (green), and series of optical sections of 0.2 μm were produced using laser scanning confocal microscopy. Formation of AJs is demonstrated between a suspended myofibroblast (encircled area) and at the dorsal membrane of a plated myofibroblast, reconstructed from three optical sections at the cell-cell interface and in z-scans performed along the indicated lines. Bar, 10 μm. (B) Reinforcement of the cortical actin of a suspended cell and insertion of stress fibers of a plated cell at contact sites is schematized. (C and D) Cell pairs were subjected to hydrodynamic shear forces, ranging from 1 to 4 Nm^{-2} and the percentage of remaining suspended cells compared with the initially seeded cell number was determined before and after steps of 1 $Nm^{-2}min^{-1}$ in control conditions (C and D, dotted lines) and in the presence of SMA-FP (5 μg/ml) (D). Note that homotypic myofibroblast pairs (M on M) exhibit higher intercellular adhesion compared with homotypic pairs of fibroblasts (F on F). SMA-FP reduces cell-cell attachment when fibroblasts were seeded onto myofibroblasts (F on M) but not in the reverse setup (M on F).

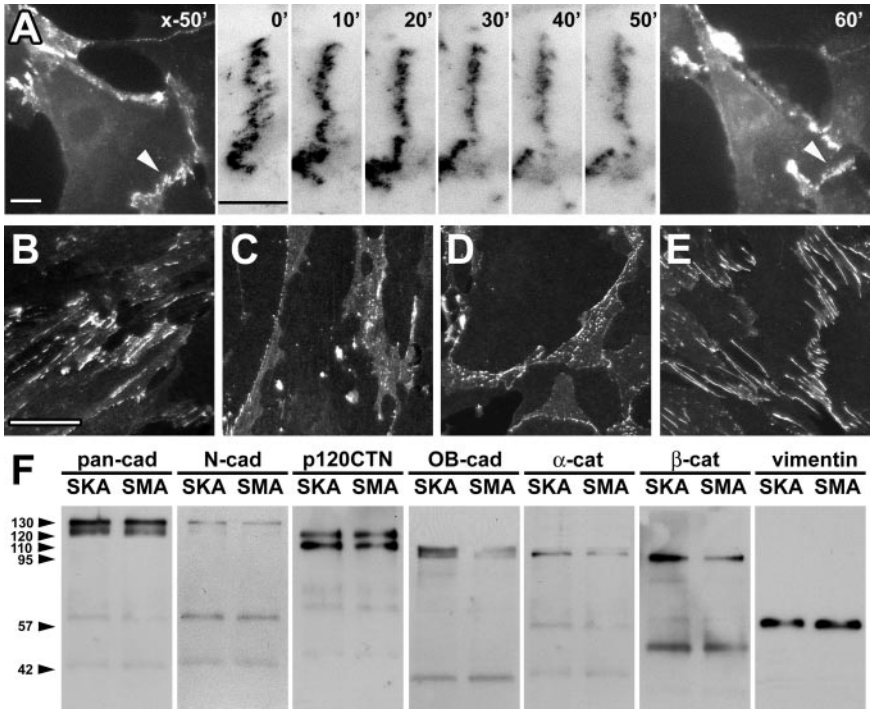

Figure 6. AJs are reinforced by α-SMA–mediated contractile activity. (A) REF-52 myofibroblasts grown on glass were transfected with EGFP-α-catenin, live recorded 50 min in control medium, and then treated with SMA-FP. Changes in AJ morphology are demonstrated for one selected cell-cell contact area (arrowheads) every 10 min in inverted fluorescence images. (B–E) LFs were treated for 2 h with control SKA-FP (B), SMA-FP (C), Y27632 (D), and LPA (E) and stained for β-catenin. Note that SMA-FP leads to reorganization of stripe-like AJs to a belt-like contact area within 30 min and induces a significant reduction of AJ formation at longer treatment, comparable with general inhibition of cell contractile activity. Bars, 25 μm. (F) Western blots compare association of AJ proteins with the TX-100–insoluble fractions of LFs after 2-h treatment with control SKA-FP (SKA) and SMA-FP (SMA).

cific disappearance of their respective target cadherin from AJs as assessed by immunofluorescence (unpublished data). Anti-N-cadherin significantly changed the morphology of fibroblast AJs (Figure 7A; Fig 7video4.mov) without having a major effect on myofibroblast contacts (unpublished data). In contrast, anti-OB-cadherin predominantly effected AJs in myofibroblasts (Figure 7B; Fig 7video5.mov) but not in fibroblasts (unpublished data) as demonstrated for EGFP-α-catenin transfected SCF (± TGFβ); control peptides were always without effect (unpublished data). Cell contraction was assessed by growing SCF in three-dimensional attached collagen lattices for 5 d (± TGFβ), where they formed AJs (Figure 7C) and by measuring gel contraction after 3 h of anti-cadherin treatment. Anti-OB-cadherin significantly inhibited contraction of myofibroblasts but not of fibroblasts compared with the respective controls (Figure 7D); anti-N-cadherin was without effect on the contraction of both cell types. To test whether the effect of anti-OB-cadherin on cell contraction is mediated by AJs, active and control anti-cadherin peptides were added to SCF (±TGFB) that were sparsely grown on deformable silicone elastomers (Hinz *et al*., 2001a); none of the peptides changed substrate wrinkle formation (unpublished data).

DISCUSSION

AJs have been described previously as electron-dense plaques that join microfilaments over the plasma membranes of contacting myofibroblasts in wound granulation tissue (Gabbiani and Rungger-Brandle, 1981; Welch *et al*., 1990); since these pioneer studies, no attempts have been made to further characterize their molecular composition and function in myofibroblasts. In contrast to cadherin-negative fibroblasts of normal dermis (Figure 8A), granulation tissue fibroblasts express cadherins, of which OB-, N-, and T-cadherin are present in considerable amounts. AJs are formed de novo ~3 d postwounding between granulation tissue proto-myofibroblasts that are characterized by α-SMA–negative stress fibers (Tomasek *et al*., 2002); proto-myofibroblasts predominantly express the classical (type I) cadherin N-cadherin (Figure 8B). Expression of N-cadherin is frequently associated with increased cell migration (Hazan *et al*., 2000), and its expression in fibroblasts during the stroma reaction to epithelial tumors may be related to invasion of epithelial cancer cells; interestingly, the invading cells similarly express N-cadherin (De Wever and Mareel, 2003). De novo expression of N-cadherin is characteristic of EMT, occurring during tumor progression and embryogenesis and is associated with cell scattering, increased cell invasiveness and lowered cell adhesion strength (Thiery, 2002). After arterial injury, up-regulation of N-cadherin in neointimal SMC was shown to correlate with the development of a fibroblastic phenotype, characterized by the loss of α-SMA expression and increased cell migration (Jones *et al*., 2002); inhibition of N-cadherin with function-blocking antibodies decreased arterial wound repair (Jones *et al*., 2002). It is tempting to speculate that in early granulation tissue N-cadherin promotes fibroblast invasion into the provisional fibrin clot matrix by inducing a migratory phenotype (Figure 8B).

Differentiated wound myofibroblasts increasingly express OB-cadherin concurrently with up-regulated α-SMA, and OB-cadherin becomes the predominant cadherin in late contractile granulation tissue (Figure 8C). OB-cadherin is an atypical (type II) member of the cadherin family, considered to be characteristic of mesenchymal cells during embryonic development (Okazaki *et al*., 1994; Kimura *et al*., 1995; Simonneau *et al*., 1995). Although OB-cadherin was originally described to be specific of osteoblasts (Okazaki *et al*., 1994), it also is expressed in adult human lung, placenta, heart, and kidney (Shibata *et al*., 1996). Interestingly, a shift from N- to OB-cadherin expression similar to that observed in granulation tissue, has been described in stroma fibroblasts reacting against human prostate cancer progression (Tomita *et al*.,

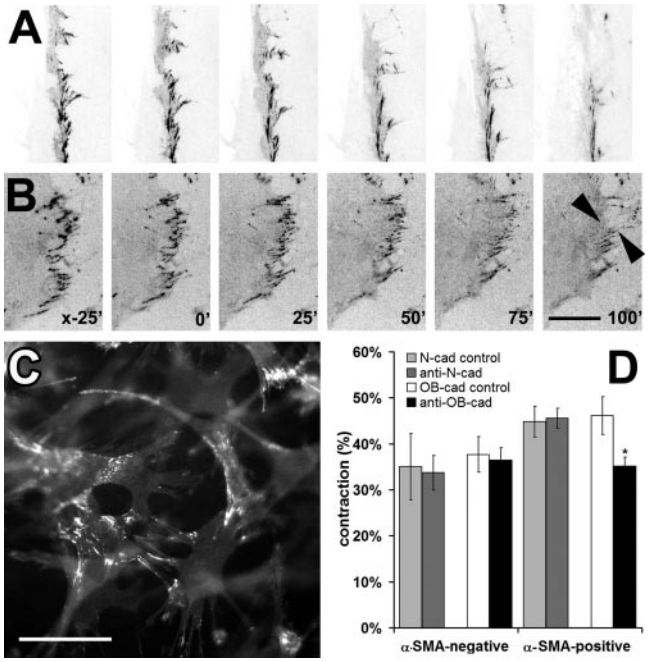

Figure 7. Formation of OB-cadherin–containing AJs increases the contraction of myofibroblast-populated collagen gels. (A) Control and (B) TGFβ-treated SCF were transfected with EGFP-α-catenin and live treated for 2 h with function-blocking peptides directed against N- (A) and OB-cadherin (B). (C) SCFs grown in three-dimensional attached collagen gels form β-catenin–positive AJs. Bars, 50 μm. (D) After 5-d culture without (α-SMA–negative) and with TGFβ (α-SMA–positive), SCFs were treated for 3 h with anti-cadherin peptides, gels were detached, and contraction was measured after 30 min; error bars indicate SD of mean (*$p \leq 0.01$, $n = 3$).

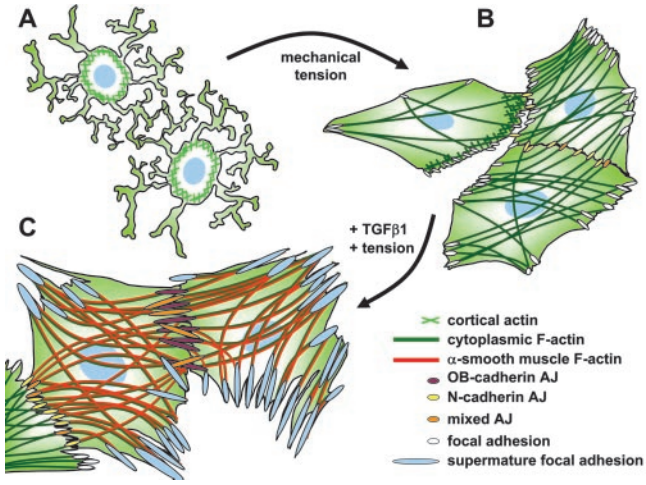

Figure 8. Model of AJ development during fibroblast to myofibroblast transition. (A) Fibroblasts in normal dermis and in mechanically unloaded three-dimensional collagen matrices exhibit a dendritic phenotype and cytoplasmic actin filaments are organized in a submembranous cortex; cells do not develop AJs but communicate via gap junctions (Salomon *et al*., 1988; Grinnell *et al*., 2003). (B) Mechanical activation by growth on rigid culture surfaces or tissue matrix reorganization during wound healing leads to the formation of α-SMA–negative stress fibers, i.e., to the development of the proto-myofibroblast (Tomasek *et al*., 2002; Hinz and Gabbiani, 2003b). Stress fibers of this migratory phenotype are connected to the ECM at sites of FAs and between cells at sites of AJs that predominantly express N-cadherin; few AJs coexpress N-cadherin and OB-cadherin. (C) TGFβ, in the presence of mechanical stress, leads to the further differentiation of myofibroblasts by inducing de novo expression of α-SMA and by increasing expression of OB-cadherin in AJs. The enhanced contractile activity mediated by α-SMA incorporation into stress fibers reinforces AJs and FAs to large supermature contact sites; AJs of differentiated myofibroblasts predominantly express OB-cadherin either exclusively or in conjunction with N-cadherin.

2000), and de novo expression of OB-cadherin was observed in fibroblasts surrounding gastric cancer cell nests (Shibata *et al*., 1996). Although these reports did not evaluate the level of α-SMA expression, fibroblasts generally differentiate into myofibroblasts during the stroma reaction to epithelial tumors (Cintorino *et al*., 1991; Ronnov-Jessen *et al*., 1996), and it is conceivable that OB-cadherin expression is confined to α-SMA–positive myofibroblasts under these conditions.

The shift from N- to OB-cadherin during wound healing is recapitulated in vitro by inducing myofibroblast differentiation with TGFβ (Figure 8C). In contrast to normal tissue fibroblasts, fibroblasts in culture form AJs and constitutively express N-cadherin (Geiger *et al*., 1990); this feature may be due to their mechanical activation on rigid culture substrates and stress fiber formation, typical of proto-myofibroblasts (Tomasek *et al*., 2002). Here, we observed a decrease in N-cadherin expression during TGFβ-induced fibroblast-to-myofibroblast transition. This is in contrast to earlier studies that reported no differences in N-cadherin levels between colon fibroblasts and myofibroblasts (Van Hoorde *et al*., 1999) and even increased levels in corneal myofibroblasts compared with their α-SMA–negative counterparts (Petridou and Masur, 1996). In contrast to the rat fibroblasts used in our study, α-SMA–negative cultured human corneal fibroblasts do not seem to form AJs (Petridou and Masur, 1996), and regulation of N-cadherin expression during corneal myofibroblast differentiation may be different from that of fibroblasts that already express considerable levels of N-cadherin in culture. Interestingly, α-SMA–positive corneal myofibroblasts also were shown to express OB-cadherin (Masur *et al*., 1999).

Besides being associated with the switch from migratory to contractile fibroblasts, the change from N- to OB-cadherin expression seems to mediate homotypic myofibroblast recognition. In aggregation assays, α-SMA–positive and –negative myofibroblasts segregate and homotypic contact formation seems to be preferred in confluent culture. In addition to the specific cadherin type, cell segregation is mediated by different activation states or amounts of cadherins in the plasma membrane (Gumbiner, 2000; Niessen and Gumbiner, 2002). Decrease of α- and β-catenin and N-cadherin expression during myofibroblast differentiation in our experiments suggests a decrease of the number of contacts. This may mediate the establishment of smaller myofibroblast aggregates compared with those formed by fibroblasts. The creation of small contractile units would theoretically contribute to a good balance of high net force and its transmission to the matrix. The role of OB-cadherin–containing AJs in increased force generation of myofibroblasts is supported by the fact that contraction of collagen gels was reduced by inhibiting OB-cadherin but not by inhibiting N-cadherin.

In addition to sustain total force development, AJs have been shown to potentially coordinate myofibroblast contractile activity and to propagate intracellular contraction signals by mechanical cell interaction. Pulling feromagnetic

bead-loaded suspended fibroblasts that have formed AJs with plated fibroblasts by means of a magnet was shown to induce Ca^{2+} transients in plated but not in suspended cells (Ko *et al*., 2001). This suggests the presence of mechanosensitive Ca^{2+} channels, whose activation requires extracellular stress and an organized actin cytoskeleton (Bershadsky *et al*., 2003); in individual migratory fibroblasts, mechanical stretching of the substrate has been shown to locally trigger Ca^{2+} influx and to increase cell (con)tractile forces (Munevar *et al*., 2004). We propose mechanical cell coupling by AJs as a mechanism to propagate Ca^{2+}signals and myofibroblast contraction in a complex three-dimensional environment. This assumption is further supported by the electrochemical coupling of cultured (Spanakis *et al*., 1998; Ko *et al*., 2000) and tissue fibroblasts via gap junctions (Salomon *et al*., 1988) that are up-regulated during wound healing (Gabbiani *et al*., 1978); inhibition of gap junctions and electrochemical uncoupling has been shown to reduce the contraction of fibroblast-populated collagen gels (Ehrlich *et al*., 2000).

To transmit the high contractile force exerted by α-SMA–positive stress fibers, AJs need to withstand considerable mechanical stress; indeed, AJs of cultured myofibroblasts are significantly larger compared with those of α-SMA–negative fibroblasts. Inducing actin-myosin based contractile activity with LPA and staurosporin reinforced AJs of fibroblasts and inhibition of contraction with a variety of drugs lead to AJ disassembly, similar to what was observed for contacting fibroblasts and epithelial cells (Gloushankova *et al*., 1998). Consequently, the activity of Rho, a central regulator of actomyosin contractile activity, was shown to reinforce AJs (Braga *et al*., 1997; Adams and Nelson, 1998; Braga, 2000), and ROCK inhibition disassembled AJs in our experiments. The contraction of fibroblasts was demonstrated to trigger a viscoelastic response in AJ-coupled adjacent fibroblasts, which is due to reorganization of the actin cytoskeleton in the contact area (Ragsdale *et al*., 1997). We here present evidence suggesting that α-SMA itself reinforces AJs by increasing intracellular tension: 1) during early spreading, when α-SMA is diffusely organized, the morphology of myofibroblast AJs is similar to that of α-SMA-negative fibroblasts; only later AJs are reinforced and elongate, analogous to the supermaturation of myofibroblast FAs (Hinz *et al*., 2003). 2) The development of larger myofibroblast AJs correlates with higher intracellular forces developed by α-SMA in stress fibers. 3) The SMA-FP decreases AJ size and mechanical resistance and 4) matrix-anchored α-SMA fibers are more efficient to provide adhesion to suspended cells under hydrodynamic flow compared with α-SMA–negative filament bundles.

Finally, cadherin-mediated signaling in the highly cellular granulation tissue of late wounds may be important to regulate the gradual loss of myofibroblast function after wound closure. Corneal myofibroblasts in dense culture significantly decrease the expression of α-SMA and dedifferentiate into α-SMA–negative fibroblasts (Masur *et al*., 1996); this has been attributed to contact-induced desensitization to TGFβ (Petridou *et al*., 2000). Interestingly, long-term homophilic engagement of E-cadherin was shown to reduce Rho activity in cultured epithelial cells (Noren *et al*., 2001; Yap and Kovacs, 2003), suggesting a role of cadherins in down-regulating cell contractile activity; however, this apparent contradiction to the role of Rho in AJ-reinforcement remains to be solved. Signaling can be mediated by the same cadherins, implicated in mechanical coupling and/or by a specialized subset of cadherins, such as T-cadherin that is considerably expressed in cultured and granulation tissue fibroblasts. T-cadherin is an unusual glycosylphosphatidylinositol-anchored cadherin that promotes weak homophilic cell binding; however, it does not localize to typical AJs when transfected into epithelial cells (Vestal and Ranscht, 1992) and the lack of a transmembrane and cytosolic domain contradicts a function in the formation of stable AJs. T-cadherin is abundant in the vascular system, in particular in arteries, exhibiting high expression in intimal SMC; fibroblasts of the adventitia are always T-cadherin–negative (Ivanov *et al*., 2001). T-cadherin gets up-regulated in medial and intimal SMC during neointima formation after experimental restenosis, suggesting a role in arterial repair (Kudrjashova *et al*., 2002). Its expression in granulation tissue may play a role in connective tissue repair; however, further studies are needed to elucidate its possible function in fibroblastic cells.

To conclude, we have demonstrated that formation of AJs and the expression level of AJ proteins increases in granulation tissue fibroblasts during wound healing and that expression shifts from N- to OB-cadherin with myofibroblast differentiation in vitro and in vivo, as summarized in Figure 8. The specificity of myofibroblast AJs leads to homotypic cell recognition and to a significant increase in the mechanical resistance of cell–cell contacts; reinforcement of AJs is provided by the high contractile activity of α-SMA. We further show that formation of OB-cadherin-type AJs in α-SMA–positive myofibroblasts, but not of N-cadherin contacts in α-SMA–negative fibroblasts, improves the contraction of a fibroblast-populated three-dimensional collagen matrix. We suggest that targeting of myofibroblast AJs by specific anti-cadherin peptides may be used to control tissue deformation in fibrotic diseases by reducing myofibroblast contraction efficiency and eventually differentiation.

ACKNOWLEDGMENTS

Drs. K. Kaibuchi (Nagoya University), C. Gauthier-Rouviere (Centre National de la Recherche Scientifiquem, Montpellier, France), V. Koteliansky (Biogen), T. Resink (University Hospital, Basel, Switzerland), J.A. Schalken (University Hospital Nijmegen, Nijmegen, The Netherlands), R.M. Mège (Institut National de la Santé et de la Recherche Médicale U440, Paris, France), and M.-L. Bochaton-Piallat (Centre Medical Universitaire, University of Geneva, Switzerland) are gratefully acknowledged for providing EGFP-α-catenin; N-cadherin-EGFP; TGFβ-sRII; anti-T-, anti-OB-, and anti-K-cadherin antibodies; and vascular SMCs, respectively. Cadherin Biomedical is acknowledged for providing high-quality anti-cadherin peptides. K. Hirano, L. Follonier, C. Grange, and A. Benattallah are acknowledged for technical assistance and Dr. H. Smola for critical reading of the manuscript. We are grateful to Dr. G. Gabbiani for constant scientific help. This work was supported by the Swiss National Science Foundation, grant #3100A0-102150/1 (to B.H.) and #3100-068313 (to C.C.).

REFERENCES

Adams, C.L., and Nelson, W.J. (1998). Cytomechanics of cadherin-mediated cell-cell adhesion. Curr. Opin. Cell Biol. *10*, 572–577.

Angst, B.D., Marcozzi, C., and Magee, A.I. (2001). The cadherin superfamily: diversity in form and function. J. Cell Sci. *114*, 629–641.

Bershadsky, A.D., Balaban, N.Q., and Geiger, B. (2003). Adhesion-dependent cell mechanosensitivity. Annu. Rev. Cell Dev. Biol. *19*, 677–695.

Bhowmick, N.A., Ghiassi, M., Bakin, A., Aakre, M., Lundquist, C.A., Engel, M.E., Arteaga, C.L., and Moses, H.L. (2001). Transforming growth factor-beta1 mediates epithelial to mesenchymal transdifferentiation through a RhoA-dependent mechanism. Mol. Biol. Cell *12*, 27–36.

Bochaton-Piallat, M.-L., Ropraz, P., Gabbiani, F., and Gabbiani, G. (1996). Phenotypic heterogeneity of rat arterial smooth muscle cell clones - implications for the development of experimental intimal thickening. Arterioscler. Thromb. Vasc. Biol. *16*, 815–820.

Braga, V. (2000). Epithelial cell shape: cadherins and small GTPases. Exp. Cell Res. *261*, 83–90.

Braga, V.M., Machesky, L.M., Hall, A., and Hotchin, N.A. (1997). The small GTPases Rho and Rac are required for the establishment of cadherin-dependent cell-cell contacts. J. Cell Biol. *137*, 1421–1431.

Chaponnier, C., Goethals, M., Janmey, P.A., Gabbiani, F., Gabbiani, G., and Vandekerckhove, J. (1995). The specific NH2-terminal sequence Ac-EEED of alpha-smooth muscle actin plays a role in polymerization in vitro and in vivo. J. Cell Biol. *130*, 887–895.

Chimori, Y., Hayashi, K., Kimura, K., Nishida, W., Funahashi, S., Miyata, S., Shimane, M., Matsuzawa, Y., and Sobue, K. (2000). Phenotype-dependent expression of cadherin 6B in vascular and visceral smooth muscle cells. FEBS Lett. *469*, 67–71.

Cintorino, M., Bellizzi de Marco, E., Leoncini, P., Tripodi, S.A., Xu, L.J., Sappino, A.P., Schmitt-Graff, A., and Gabbiani, G. (1991). Expression of alpha-smooth-muscle actin in stromal cells of the uterine cervix during epithelial neoplastic changes. Int. J. Cancer *47*, 843–846.

Darby, I., Skalli, O., and Gabbiani, G. (1990). Alpha-smooth muscle actin is transiently expressed by myofibroblasts during experimental wound healing. Lab. Investig. *63*, 21–29.

De Wever, O., and Mareel, M. (2003). Role of tissue stroma in cancer cell invasion. J. Pathol. *200*, 429–447.

Derossi, D., Joliot, A.H., Chassaing, G., and Prochiantz, A. (1994). The third helix of the Antennapedia homeodomain translocates through biological membranes. J. Biol. Chem. *269*, 10444–10450.

Desmouliere, A., Geinoz, A., Gabbiani, F., and Gabbiani, G. (1993). Transforming growth factor-beta 1 induces alpha-smooth muscle actin expression in granulation tissue myofibroblasts and in quiescent and growing cultured fibroblasts. J. Cell Biol. *122*, 103–111.

Dugina, V., Fontao, L., Chaponnier, C., Vasiliev, J., and Gabbiani, G. (2001). Focal adhesion features during myofibroblastic differentiation are controlled by intracellular and extracellular factors. J. Cell Sci. *114*, 3285–3296.

Ehrlich, H.P., Gabbiani, G., and Meda, P. (2000). Cell coupling modulates the contraction of fibroblast-populated collagen lattices. J. Cell. Physiol. *184*, 86–92.

Fukata, M., Nakagawa, M., Itoh, N., Kawajiri, A., Yamaga, M., Kuroda, S., and Kaibuchi, K. (2001). Involvement of IQGAP1, an effector of Rac1 and Cdc42 GTPases, in cell-cell dissociation during cell scattering. Mol. Cell. Biol. *21*, 2165–2183.

Gabbiani, G., Chaponnier, C., and Huttner, I. (1978). Cytoplasmic filaments and gap junctions in epithelial cells and myofibroblasts during wound healing. J. Cell Biol. *76*, 561–568.

Gabbiani, G., and Rungger-Brandle, E. (1981). Tissue Repair and Regeneration. In: Handbook of Inflammation, ed. L.E. Glynn, Amsterdam, The Netherlands: Elsevier, 1–50.

Gabbiani, G., Ryan, G.B., and Majno, G. (1971). Presence of modified fibroblasts in granulation tissue and their possible role in wound contraction. Experientia *27*, 549–550.

Geiger, B., Volberg, T., Ginsberg, D., Bitzur, S., Sabanay, I., and Hynes, R.O. (1990). Broad spectrum pan-cadherin antibodies, reactive with the C-terminal 24 amino acid residues of N-cadherin. J. Cell Sci. *97*, 607–614.

Gloushankova, N.A., Krendel, M.F., Alieva, N.O., Bonder, E.M., Feder, H.H., Vasiliev, J.M., and Gelfand, I.M. (1998). Dynamics of contacts between lamellae of fibroblasts: essential role of the actin cytoskeleton. Proc. Natl. Acad. Sci. USA *95*, 4362–4367.

Grinnell, F., Ho, C.H., Tamariz, E., Lee, D.J., and Skuta, G. (2003). Dendritic fibroblasts in three-dimensional collagen matrices. Mol. Biol. Cell *14*, 384–395.

Gumbiner, B.M. (2000). Regulation of cadherin adhesive activity. J. Cell Biol. *148*, 399–404.

Hatta, K., and Takeichi, M. (1986). Expression of N-cadherin adhesion molecules associated with early morphogenetic events in chick development. Nature *320*, 447–449.

Hazan, R.B., Phillips, G.R., Qiao, R.F., Norton, L., and Aaronson, S.A. (2000). Exogenous expression of N-cadherin in breast cancer cells induces cell migration, invasion, and metastasis. J. Cell Biol. *148*, 779–790.

Hinz, B., Celetta, G., Tomasek, J.J., Gabbiani, G., and Chaponnier, C. (2001a). Alpha-smooth muscle actin expression upregulates fibroblast contractile activity. Mol. Biol. Cell *12*, 2730–2741.

Hinz, B., Dugina, V., Ballestrem, C., Wehrle-Haller, B., and Chaponnier, C. (2003). α-Smooth muscle actin is crucial for focal adhesion maturation in myofibroblasts. Mol. Biol. Cell *14*, 2508–2519.

Hinz, B., and Gabbiani, G. (2003a). Cell-matrix and cell-cell contacts of myofibroblasts: role in connective tissue remodeling. Thromb. Haemost. *90*, 993–1002.

Hinz, B., and Gabbiani, G. (2003b). Mechanisms of force generation and transmission by myofibroblasts. Curr. Opin. Biotechnol. *14*, 538–546.

Hinz, B., Gabbiani, G., and Chaponnier, C. (2002). The NH2-terminal peptide of alpha-smooth muscle actin inhibits force generation by the myofibroblast in vitro and in vivo. J. Cell Biol. *157*, 657–663.

Hinz, B., Mastrangelo, D., Iselin, C.E., Chaponnier, C., and Gabbiani, G. (2001b). Mechanical tension controls granulation tissue contractile activity and myofibroblast differentiation. Am. J. Pathol. *159*, 1009–1020.

Hoffmann, I., and Balling, R. (1995). Cloning and expression analysis of a novel mesodermally expressed cadherin. Dev. Biol. *169*, 337–346.

Ivanov, D., Philippova, M., Antropova, J., Gubaeva, F., Iljinskaya, O., Tararak, E., Bochkov, V., Erne, P., Resink, T., and Tkachuk, V. (2001). Expression of cell adhesion molecule T-cadherin in the human vasculature. Histochem. Cell Biol. *115*, 231–242.

Jones, M., Sabatini, P.J., Lee, F.S., Bendeck, M.P., and Langille, B.L. (2002). N-cadherin upregulation and function in response of smooth muscle cells to arterial injury. Arterioscler. Thromb. Vasc. Biol. *22*, 1972–1977.

Kimura, Y., Matsunami, H., Inoue, T., Shimamura, K., Uchida, N., Ueno, T., Miyazaki, T., and Takeichi, M. (1995). Cadherin-11 expressed in association with mesenchymal morphogenesis in the head, somite, and limb bud of early mouse embryos. Dev. Biol. *169*, 347–358.

Ko, K., Arora, P., Lee, W., and McCulloch, C. (2000). Biochemical and functional characterization of intercellular adhesion and gap junctions in fibroblasts. Am. J. Physiol. *279*, C147–C157.

Ko, K.S., Arora, P.D., and McCulloch, C.A. (2001). Cadherins mediate intercellular mechanical signaling in fibroblasts by activation of stretch-sensitive calcium-permeable channels. J. Biol. Chem. *276*, 35967–35977.

Kudrjashova, E., *et al*. (2002). Expression of adhesion molecule T-cadherin is increased during neointima formation in experimental restenosis. Histochem. Cell Biol. *118*, 281–290.

Malmstrom, J., *et al*. (2004). Transforming growth factor-beta 1 specifically induce proteins involved in the myofibroblast contractile apparatus. Mol. Cell Proteomics *3*, 466–477.

Marthiens, V., Padilla, F., Lambert, M., and Mege, R.M. (2002). Complementary expression and regulation of cadherins 6 and 11 during specific steps of motoneuron differentiation. Mol. Cell Neurosci. *20*, 458–475.

Mary, S., Charrasse, S., Meriane, M., Comunale, F., Travo, P., Blangy, A., and Gauthier-Rouviere, C. (2002). Biogenesis of N-cadherin-dependent cell-cell contacts in living fibroblasts is a microtubule-dependent kinesin-driven mechanism. Mol. Biol. Cell *13*, 285–301.

Masur, S.K., Conors, R.J., Jr., Cheung, J.K., and Antohi, S. (1999). Matrix adhesion characteristics of corneal myofibroblasts. Investig. Ophthalmol. Vis. Sci. *40*, 904–910.

Masur, S.K., Dewal, H.S., Dinh, T.T., Erenburg, I., and Petridou, S. (1996). Myofibroblasts differentiate from fibroblasts when plated at low density. Proc. Natl. Acad. Sci. USA *93*, 4219–4223.

Matsuyoshi, N., and Imamura, S. (1997). Multiple cadherins are expressed in human fibroblasts. Biochem. Biophys. Res. Commun. *235*, 355–358.

Miettinen, P.J., Ebner, R., Lopez, A.R., and Derynck, R. (1994). TGF-beta induced transdifferentiation of mammary epithelial cells to mesenchymal cells: involvement of type I receptors. J. Cell Biol. *127*, 2021–2036.

Moiseeva, E.P. (2001). Adhesion receptors of vascular smooth muscle cells and their functions. Cardiovasc. Res. *52*, 372–386.

Munevar, S., Wang, Y.L., and Dembo, M. (2004). Regulation of mechanical interactions between fibroblasts and the substratum by stretch-activated Ca2+ entry. J. Cell Sci. *117*, 85–92.

Nagafuchi, A. (2001). Molecular architecture of adherens junctions. Curr. Opin. Cell Biol. *13*, 600–603.

Niermann, T., Schmutz, S., Erne, P., and Resink, T. (2003). Aryl hydrocarbon receptor ligands repress T-cadherin expression in vascular smooth muscle cells. Biochem. Biophys. Res. Commun. *300*, 943–949.

Niessen, C.M., and Gumbiner, B.M. (2002). Cadherin-mediated cell sorting not determined by binding or adhesion specificity. J. Cell Biol. *156*, 389–399.

Noren, N.K., Niessen, C.M., Gumbiner, B.M., and Burridge, K. (2001). Cadherin engagement regulates Rho family GTPases. J. Biol. Chem. *276*, 33305–33308.

Okazaki, M., Takeshita, S., Kawai, S., Kikuno, R., Tsujimura, A., Kudo, A., and Amann, E. (1994). Molecular cloning and characterization of OB-cadherin, a new member of cadherin family expressed in osteoblasts. J. Biol. Chem. *269*, 12092–12098.

Omelchenko, T., Fetisova, E., Ivanova, O., Bonder, E.M., Feder, H., Vasiliev, J.M., and Gelfand, I.M. (2001). Contact interactions between epitheliocytes and fibroblasts: formation of heterotypic cadherin-containing adhesion sites is accompanied by local cytoskeletal reorganization. Proc. Natl. Acad. Sci. USA *98*, 8632–8637.

Orlandini, M., and Oliviero, S. (2001). In fibroblasts Vegf-D expression is induced by cell-cell contact mediated by cadherin-11. J. Biol. Chem. *276*, 6576–6581.

Petridou, S., Maltseva, O., Spanakis, S., and Masur, S.K. (2000). TGF-beta receptor expression and smad2 localization are cell density dependent in fibroblasts. Invest. Ophthalmol. Vis. Sci. *41*, 89–95.

Petridou, S., and Masur, S.K. (1996). Immunodetection of connexins and cadherins in corneal fibroblasts and myofibroblasts. Investig. Ophthalmol. Vis. Sci. *37*, 1740–1748.

Ragsdale, G.K., Phelps, J., and Luby-Phelps, K. (1997). Viscoelastic response of fibroblasts to tension transmitted through adherens junctions. Biophys. J. *73*, 2798–2808.

Ronnov-Jessen, L., and Petersen, O.W. (1993). Induction of alpha-smooth muscle actin by transforming growth factor-beta 1 in quiescent human breast gland fibroblasts. Implications for myofibroblast generation in breast neoplasia. Lab. Investig. *68*, 696–707.

Ronnov-Jessen, L., Petersen, O.W., and Bissell, M.J. (1996). Cellular changes involved in conversion of normal to malignant breast: importance of the stromal reaction. Physiol. Rev. *76*, 69–125.

Rosenberg, P., Esni, F., Sjodin, A., Larue, L., Carlsson, L., Gullberg, D., Takeichi, M., Kemler, R., and Semb, H. (1997). A potential role of R-cadherin in striated muscle formation. Dev. Biol. *187*, 55–70.

Salomon, D., Saurat, J.H., and Meda, P. (1988). Cell-to-cell communication within intact human skin. J. Clin. Investig. *82*, 248–254.

Serini, G., and Gabbiani, G. (1999). Mechanisms of myofibroblast activity and phenotypic modulation. Exp. Cell Res. *250*, 273–283.

Shibata, T., Ochiai, A., Gotoh, M., Machinami, R., and Hirohashi, S. (1996). Simultaneous expression of cadherin-11 in signet-ring cell carcinoma and stromal cells of diffuse-type gastric cancer. Cancer Lett. *99*, 147–153.

Shimoyama, Y., Tsujimoto, G., Kitajima, M., and Natori, M. (2000). Identification of three human type-II classic cadherins and frequent heterophilic interactions between different subclasses of type-II classic cadherins. Biochem. J. *349*, 159–167.

Shin, C.S., Lecanda, F., Sheikh, S., Weitzmann, L., Cheng, S.L., and Civitelli, R. (2000). Relative abundance of different cadherins defines differentiation of mesenchymal precursors into osteogenic, myogenic, or adipogenic pathways. J. Cell Biochem. *78*, 566–577.

Simonneau, L., Kitagawa, M., Suzuki, S., and Thiery, J.P. (1995). Cadherin 11 expression marks the mesenchymal phenotype: towards new functions for cadherins? Cell Adhes. Commun. *3*, 115–130.

Singer, I.I., Kawka, D.W., Kazazis, D.M., and Clark, R.A. (1984). In vivo co-distribution of fibronectin and actin fibers in granulation tissue: immunofluorescence and electron microscope studies of the fibronexus at the myofibroblast surface. J. Cell Biol. *98*, 2091–2106.

Skalli, O., Ropraz, P., Trzeciak, A., Benzonana, G., Gillessen, D., and Gabbiani, G. (1986). A monoclonal antibody against alpha-smooth muscle actin: a new probe for smooth muscle differentiation. J. Cell Biol. *103*, 2787–2796.

Spanakis, S.G., Petridou, S., and Masur, S.K. (1998). Functional gap junctions in corneal fibroblasts and myofibroblasts. Investig. Ophthalmol. Vis. Sci. *39*, 1320–1328.

Thiery, J.P. (2002). Epithelial-mesenchymal transitions in tumour progression. Nat. Rev. Cancer *2*, 442–454.

Tomasek, J.J., Gabbiani, G., Hinz, B., Chaponnier, C., and Brown, R.A. (2002). Myofibroblasts and mechano-regulation of connective tissue remodelling. Nat. Rev. Mol. Cell. Biol. *3*, 349–363.

Tomita, K., van Bokhoven, A., van Leenders, G.J., Ruijter, E.T., Jansen, C.F., Bussemakers, M.J., and Schalken, J.A. (2000). Cadherin switching in human prostate cancer progression. Cancer Res. *60*, 3650–3654.

Van Hoorde, L., Braet, K., and Mareel, M. (1999). The N-cadherin/catenin complex in colon fibroblasts and myofibroblasts. Cell Adhes. Commun. *7*, 139–150.

Vestal, D.J., and Ranscht, B. (1992). Glycosyl phosphatidylinositol–anchored T-cadherin mediates calcium-dependent, homophilic cell adhesion. J. Cell Biol. *119*, 451–461.

Volk, T., Cohen, O., and Geiger, B. (1987). Formation of heterotypic adherens-type junctions between L-CAM-containing liver cells and A-CAM-containing lens cells. Cell *50*, 987–994.

Welch, M.P., Odland, G.F., and Clark, R.A. (1990). Temporal relationships of F-actin bundle formation, collagen and fibronectin matrix assembly, and fibronectin receptor expression to wound contraction. J. Cell Biol. *110*, 133–145.

Wheelock, M.J., and Johnson, K.R. (2003). Cadherins as modulators of cellular phenotype. Annu. Rev. Cell Dev. Biol. *19*, 207–235.

Yap, A.S., and Kovacs, E.M. (2003). Direct cadherin-activated cell signaling: a view from the plasma membrane. J. Cell Biol. *160*, 11–16.

Yonemura, S., Itoh, M., Nagafuchi, A., and Tsukita, S. (1995). Cell-to-cell adherens junction formation and actin filament organization: similarities and differences between non-polarized fibroblasts and polarized epithelial cells. J. Cell Sci. *108*, 127–142.